DALTON
FULL PAPER

Kinetics and mechanism of the chromium(VI) oxidation of methyl α-D-glucopyranoside and methyl α-D-mannopyranoside †

Sandra Signorella,[a] María Inés Frascaroli,[a] Silvia García,[a] Mabel Santoro,[a] Juan Carlos González,[a] Claudia Palopoli,[a] Verónica Daier,[a] Nieves Casado[b] and Luis F. Sala *[a]

[a] *Departamento de Química, Facultad de Ciencias Bioquímicas y Farmacéuticas, UNR, Suipacha 531, 2000 Rosario, Argentina. E-mail: inquibir@satlink.com; Fax: ++54 341 4350214*
[b] *Instituto de Desarrollo Tecnológico para la Industria Química, Güemes 3450, 3000 Santa Fe, Argentina*

Received 21st October 1999, Accepted 22nd February 2000
Published on the Web 20th April 2000

The oxidation of methyl α-D-glucopyranoside (Glc1Me) and methyl α-D-mannopyranoside (Man1Me) by Cr^{VI} yielded Cr^{3+} and methyl α-D-glycofuranurono-6,3-lactone as final products when an excess of the methyl glycoside over Cr^{VI} was used. The redox reaction occurs through $Cr^{VI} \longrightarrow Cr^{IV} \longrightarrow Cr^{III}$ and $Cr^{VI} \longrightarrow Cr^{V} \longrightarrow Cr^{III}$ paths, the Cr^{VI}/Cr^{IV} reduction being the slow redox step. The complete rate laws for the redox reactions are expressed by: $-d[Cr^{VI}]/dt = k_{GH}[H^+]^2[Glc1Me][Cr^{VI}]$, where $k_{GH} = (6.75 \pm 0.05) \times 10^{-3}$ M^{-3} s^{-1}; and $-d[Cr^{VI}]/dt = (k_{M0} + k_{MH}[H^+]^2)[Man1Me][Cr^{VI}]$, where $k_{M0} = (5 \pm 1) \times 10^{-4}$ M^{-1} s^{-1} and $k_{MH} = (6.5 \pm 0.2) \times 10^{-3}$ M^{-3} s^{-1}, at 40 °C. In acid medium, intermediate Cr^{V} reacts with the substrate faster than Cr^{VI} does. Chromium(V) mono- and bis-chelates were detected by EPR spectroscopy, and the EPR spectra show that the distribution of these species essentially depends on the solution acidity.

Introduction

Chromium is a well known genotoxic and carcinogenic metal.[1–3] The biological reduction of Cr^{VI} to lower states has been observed with a wide variety of naturally occurring cellular reductants.[4–8] Ligands that possess two oxygen atoms able to form five-membered rings about the metal ion, such as 1,2-diols and α-hydroxyacids, are effective as non-enzymatic reductants and complexation agents towards hypervalent chromium and can stabilise the labile oxidation states of chromium.[9–15] For this reason, it is interesting to look at the ability of monosaccharides and their derivatives to reduce Cr^{VI} to Cr^{III}, in order to know the role they may play in the chemistry of Cr^{VI}.

We have previously examined the reactions of Cr^{VI} with low-molecular-weight molecules.[16–28] Our previous studies on the reduction of Cr^{VI} by aldoses[16,26,27] and deoxyaldoses[16,19,21,26,27] afforded information about the relative abilities of these monosaccharides to reduce chromate and the steric factors influencing the rate of oxidation of monosaccharides by Cr^{VI} and by the intermediate Cr^{V} formed during the reaction course.[27,28] For all the studied aldoses, the C1–OH hemiacetalic function reacts faster than the primary or any of the secondary alcoholic groups, and the aldonic acid (or/and the corresponding lactone) is the only reaction product when a tenfold or higher aldose to Cr^{VI} ratio is used. In nature, a vast number of glycosides occur in the form of glycopyranosyl and glycofuranosyl attachments to aglycones. They are present in all plants and include a large group of phenolic glycosides, the *C*-glycosyl compounds, the thioglycosides, the physiologically important cardiac glycosides, plant pigments and many others.[29–32] However, the reactivity, selectivity and mechanism of the chromium(VI) oxidation of sugars where the anomeric position is protected are not known. Methyl glycosides are the simplest sugar derivatives to evaluate the influence of blocking the anomeric position of the monosaccharide on oxidation by Cr^{VI}. In this work, we study the chromium(VI) oxidation of methyl α-D-mannopyranoside (Man1Me) and methyl α-D-glucopyranoside (Glc1Me) (Scheme 1), and provide information on the factors influencing the reaction kinetics and mechanism as well as on the structure of the intermediate chromium(V) species.

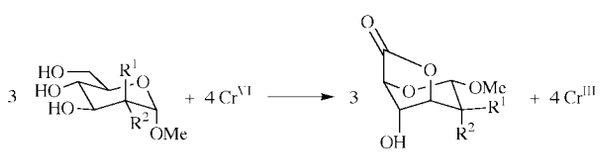

$R^1 = H, R^2 = OH$ Glc1Me methyl α-D-glucofuranurono-6,3-lactone
$R^1 = OH, R^2 = H$ Man1Me methyl α-D-mannofuranurono-6,3-lactone

Scheme 1

Experimental

Materials

Methyl α-D-glucopyranoside (Sigma grade), methyl α-D-mannopyranoside (Sigma grade), potassium dichromate (Mallinckrodt), perchloric acid (A.C.S. Baker), sulfuric acid (Merck), acrylonitrile (Aldrich grade) and sodium hydroxide (Cicarelli p. a.) were used without further purification. Water was purified by deionisation, followed by double distillation from a potassium permanganate solution.

For experiments performed in the 1–5 pH range, the pH of the solutions was adjusted by addition of 0.5 M $HClO_4$. In experiments performed at constant ionic strength ($I = 1.0$ M) and different hydrogen ion concentrations, mixtures of sodium perchlorate solutions and perchloric acid solutions were used. Sodium perchlorate solutions were prepared from sodium hydroxide and perchloric acid solutions. The concentration of stock solutions of perchloric acid was determined by titration employing standard analytical methods.[33]

CAUTION: chromic acids and acrylonitrile are toxic and carcinogens.

† Electronic supplementary information (ESI) available: time dependent UV-Vis spectra of the reaction mixtures. See http://www.rsc.org/suppdata/dt/a9/a908410j/

DOI: 10.1039/a908410j

Methods

Product analysis. Under the conditions used in the kinetic measurements (excess of methyl glycoside over Cr^{VI}), the methyl glycofuranurono-6,3-lactone was identified as the only reaction product by HPLC. The chromatograms were obtained on a KNK-500 A chromatograph provided with a 7125 HPLC pump. The separation was carried out on an Aminex HPX-87H HPLC column (300 × 7.8 mm, Bio-Rad Laboratories) using 4.5×10^{-3} M H_2SO_4 as eluent and a flow rate of 0.5 ml min^{-1}, at 26 °C. The effluent was monitored with a refractive index detector (ERC-7522, ERMA INC). The standard solutions and the reaction mixture samples were filtered through a 0.22 μm membrane prior to the injection into the chromatographic system.

Standard solutions of the methyl D-glycopyranosides, methyl D-glycofuranurono-6,3-lactone and D-glycuronic acid (and its lactone) were prepared individually in 0.5 M $HClO_4$ and chromatographed separately in order to determine the retention time of each sample. The peak corresponding to the methyl glycofuranurono-6,3-lactone was found to decrease in intensity with time while two new peaks appeared and became the dominant features of the chromatogram. These two peaks were found to correspond to the glycuronic acid in equilibrium with the corresponding glycuronolactone.

In a typical experiment, a reaction mixture containing 8×10^{-4} M Cr^{VI} and 0.016 M Glc1Me in 0.5 M $HClO_4$ was chromatographed. The methyl α-D-glucofuranurono-6,3-lactone was the only detected reaction product and it was identified by comparison against an authentic sample synthesized according to a described method.[34] As in the case of the standard sample of the methyl D-glucofuranurono-6,3-lactone, the reaction product partially hydrolyses and chromatograms run at different times after the end of the reaction show two additional peaks corresponding to D-glucuronic acid and D-glucuronolactone.

Alternatively, the possible formation of the methyl α-D-gluco-hexodialdo-6,3-furanose-1,5-pyranoside as the reaction product was tested by addition of 2,4-dinitrophenylhydrazine to the Cr^{VI}/Glc1Me reaction mixture. The 2,4-dinitrophenylhydrazone derivative was not observed. The same test was made on the reaction mixture of Ce^{IV} and Glc1Me which yields the α-D-gluco-hexodialdo-6,3-furanose-1,5-pyranoside as the reaction product.[35] In this case, the 2,4-dinitrophenylhydrazone derivative was detected and identified by the characteristic absorbance bands at 420 and 520 nm.[36]

At the methyl glycosides to Cr^{VI} ratios used in the kinetic studies, carbon dioxide was never detected as a reaction product.

Glycosides stability. The stability of Glc1Me and Man1Me under conditions used in the kinetic studies was checked by monitoring the optical rotation changes on a JENA polarimeter with thermostatted 20 cm tubes using the sodium D line. Reactant solutions were previously thermostatted and transferred to the cell immediately after mixing and the optical rotations registered at different times after the preparation of the solutions are identical to those of the freshly prepared Glc1Me and Man1Me solutions. The specific rotation of Glc1Me and Man1Me were found to be $[a]_D^{40} = +155.5 \pm 0.5$ deg cm^3 g^{-1} dm^{-1} ($c = 0.7$ M, 1.0 M $HClO_4$, $t = 5$ to 1710 min) and $[a]_D^{40} = +70.5 \pm 0.5$ deg cm^3 g^{-1} dm^{-1} ($c = 0.56$ M, 1.0 M $HClO_4$, $t = 5$ to 1440 min), respectively.

Polymerisation test. The presence of free radicals was tested for the reaction of the methyl glycoside (Gly1Me) with Cr^{VI}. In a typical experiment, to a solution of $K_2Cr_2O_7$ (0.004 mmol) and Glc1Me (or Man1Me) (0.8 mmol) in 4 ml of 1.0 M $HClO_4$ was added 1 ml of acrylonitrile in 1.0 M $HClO_4$ (1 : 1) at 40 °C. After a few minutes a white precipitate appeared. Control experiments (without $K_2Cr_2O_7$ or reductant present) did not show the formation of a precipitate.

Spectrophotometric measurements. Kinetics measurements were made by monitoring the absorbance changes on a JASCO V-530 spectrophotometer with fully thermostatted cell compartments. The reactions were followed under pseudo-first-order conditions, using at least a 300-fold excess of glycoside over Cr^{VI}. Reactant solutions were previously thermostatted and transferred to a cell of 1 cm path length immediately after mixing. Experiments were performed at 40 °C unless otherwise mentioned.

Disappearance of Cr^{VI} was followed at 350 nm until at least 80% conversion. In most experiments the concentration of Cr^{VI} was kept constant at 6×10^{-4} while the glycoside concentration was varied from 0.18 to 0.48 M. The observed pseudo-first-order rate constants (k_{obs}), determined from the slopes of the linear part of plots of ln (A_{350}) *vs.* time, were deduced from multiple determinations and were within ±10% of each other. The first-order dependence of the rate upon [Cr^{VI}] was verified. The k_{obs} were calculated at various $[Cr^{VI}]_0$, but at constant temperature, initial glycoside concentration, acidity and ionic strength. As expected on the basis of the rate law $-d(\ln[Cr^{VI}])/dt = k_{obs}$, where $k_{obs} = f([\text{glycoside}][H^+])$, k_{obs} was found to be essentially constant with increasing $[Cr^{VI}]_0$.

At the end of the reaction of Cr^{VI} with Glc1Me the two d–d bands ascribed to Cr^{III} were observed at $\lambda_{max} = 409$ ($\varepsilon = 18$) and 574 nm ($\varepsilon = 15.3$ dm^3 mol^{-1} cm^{-1}). Both, visible and UV spectral maxima and intensities, are in close agreement with those observed for the $[Cr(H_2O)_6]^{3+}$ ion. At the end of the reaction of Cr^{VI} with Man1Me the two chromium(III) d–d bands were also observed at $\lambda_{max} = 409$ and 574 nm but with higher absorbance than expected for the total $[Cr(H_2O)_6]^{3+}$ formed in the reaction. The intensity of these d–d bands decreased with time toward the two bands with the molar absorption coefficients corresponding to the $[Cr(H_2O)_6]^{3+}$ ion. This behaviour had previously been observed when a chromium(III) complex formed as the final redox product and then hydrolysed to the Cr^{3+} ion.[25,37]

The formation of Cr^{III} was monitored by following changes in the 570 nm absorption band. In these experiments the $[Cr^{VI}]_0$ was kept constant at 0.02 M, the [H^+] was varied between 0.6 and 1.0 M, and two different glycoside concentrations (0.36 and 0.46 M) were used. Under these conditions, the first-order dependence of the rate upon [Cr^{VI}] was verified and k_{obs} were obtained by following the decay of Cr^{II} at 500 nm (we checked that Cr^{VI} obeys Beer's law at this wavelength in the range of concentrations 0.01 to 0.03 M). Initial reaction rates were obtained by fitting the absorbance (500 and 570 nm)–time data by a polynomial expression[38] and calculating the slope of the tangent at time zero (r_i). First-order rate constants were obtained from these initial rates using the equation $-r_i/(A_0 - A_f)$, with average values of the initial rate (r_i) and calculated estimates of ($A_0 - A_f$).

EPR Measurements. The EPR spectra were obtained on a Bruker ESP 300 E spectrometer. The microwave frequency was generated with a Bruker 04 ER (9–10 GHz) and measured with a Racal-Dana frequency meter. The magnetic field was measured with a Bruker NMR-probe gaussmeter. All of the EPR experiments were carried out at room temperature. Spectra were simulated using the program PEST WinSIM,[39] using 100% Lorentzian lineshapes.

Results

Rate studies

Over the whole range of perchloric acid concentrations used in the kinetic measurements, spectrophotometric studies showed that the reaction of Glc1Me (or Man1Me) with Cr^{VI} resulted in an absorbance band at 350 nm and a shoulder at 420–500 nm characteristic of the chromium(VI) ion. It is known that chromium(V) species, usually formed in these oxidation reac-

Table 1 Observed pseudo-first-order rate constants (k_{obs}) for different concentrations of $HClO_4$ and methyl glycoside. $T = 40$ °C; $[Cr^{VI}]_0 = 6 \times 10^{-4}$ M; $I = 1$ M

	$10^4\ k_{obs}/s^{-1}$ at $[HClO_4]$/M					
	0.3	0.45	0.6	0.75	0.9	1.0
[Man1Me]/M						
0.18	1.9 ± 0.2	3.3 ± 0.2	5.4 ± 0.4	7.5 ± 0.3	—	12 ± 1
0.24	2.2 ± 0.2	4.3 ± 0.1	6.8 ± 0.6	10 ± 1	—	17 ± 1
0.30	3.1 ± 0.3	5.4 ± 0.5	8.8 ± 0.7	12 ± 1	16 ± 1	21 ± 2
0.36	3.4 ± 0.3	6.4 ± 0.6	10 ± 1	15 ± 1	20 ± 2	25 ± 1
0.42	4.3 ± 0.4	7.7 ± 0.3	12 ± 1	17 ± 1	23 ± 2	—
0.48	4.9 ± 0.5	8.7 ± 0.4	14 ± 1	20 ± 1	26 ± 2	34 ± 3
[Glc1Me]/M						
0.18	1.12 ± 0.01	2.53 ± 0.02	4.52 ± 0.01	7.08 ± 0.03	9.66 ± 0.02	12.3 ± 0.1
0.24	1.49 ± 0.02	3.30 ± 0.03	5.90 ± 0.01	9.00 ± 0.05	13.5 ± 0.2	16.2 ± 0.1
0.30	1.87 ± 0.01	4.27 ± 0.01	7.59 ± 0.06	11.9 ± 0.1	16.2 ± 0.1	20.6 ± 0.1
0.36	2.25 ± 0.04	5.08 ± 0.01	8.70 ± 0.01	13.7 ± 0.1	19.5 ± 0.3	23.5 ± 0.1
0.42	2.65 ± 0.04	6.05 ± 0.03	10.8 ± 0.1	16.6 ± 0.2	22.8 ± 0.1	29.1 ± 0.1
0.48	3.01 ± 0.01	7.02 ± 0.07	11.9 ± 0.1	18.7 ± 0.1	26.0 ± 0.1	31.3 ± 0.3

tions, absorb at 350 nm and may superimpose chromium(VI) absorbance yielding the wrong interpretation of spectrophotometric absorbance decay values.[40] However, if Cr^V reacts faster than Cr^{VI} and exists in solution in a sufficiently small concentration, changes in absorbance at 350 nm essentially reflect changes in chromium(VI) concentration. We observed deviations from first-order decay over very short time periods and calculated pseudo-first-order rate constants from the slopes of the linear part of the ln(*A*) *vs.* time curves, a good criterion only if Cr^V decays faster than Cr^{VI}. In order to evaluate the relative values of the Cr^{VI} *vs.* Cr^V reduction rates (k_6 *vs.* k_5) we compared the chromium(V) EPR signal intensity variation to the rate of the chromium(VI) consumption, and found that $k_5 \gg k_6$, in the range of $[H^+]$ used in the kinetic measurements. Besides, we followed the formation of Cr^{III} at 570 nm in the 0.6–1.0 M $HClO_4$ concentration range in order to determine the rate of chromium(III) formation relative to that of the chromium(VI) consumption. The k_{obs} values obtained at this wavelength are coincident with those obtained from the chromium(VI) decay at 350 nm, with the same dependence on $[H^+]$. This means that Cr^{III} forms as fast as Cr^{VI} is consumed and that the slow redox path effectively implies the reduction of Cr^{VI}, which should react slower than Cr^V does. This is also consistent with the observation of isosbestic points at 525 and 529 nm for the reaction of Cr^{VI} with Man1Me (Fig. S1) and Glc1Me (Fig. S2, ESI data),† respectively, and implies a low $[Cr^V]$ throughout the reaction when $[H^+] > 0.1$ M is used.

Table 1 summarises values of k_{obs} for various concentrations of Man1Me at different concentrations of $HClO_4$. Plots of k_{obs} *vs.* [Man1Me] (Fig. 1) gave good straight lines with zero intercept from which values of k_M were determined (Table 2). Fig. 1 (inset) shows the dependence of k_M on $[HClO_4]$, which may be expressed as in eqn. (1), where $k_{M0} = (5 \pm 1) \times 10^{-4}\ M^{-1}\ s^{-1}$ and

$$k_M = k_{M0} + k_{MH}\,[H^+]^2 \qquad (1)$$

$k_{MH} = (6.5 \pm 0.2) \times 10^{-3}\ M^{-3}\ s^{-1}$. The complete rate law for the reaction of Man1Me and Cr^{VI} is then given by eqn. (2) where $[Cr^{VI}]_T$ represents the total chromium(VI) concentration.

$$-d[Cr^{VI}]/dt = k_{obs}\,[Cr^{VI}]_T = \{k_{M0} + k_{MH}\,[H^+]^2\}[Man1Me]\,[Cr^{VI}]_T \qquad (2)$$

For the oxidation of Glc1Me, plots of k_{obs} (Table 1) *vs.* [Glc1Me] (Fig. 2) gave straight lines with zero intercept from which values of k_G were determined (Table 2). The dependence of the second-order rate constant k_G on acidity is shown in Fig. 2 (inset) and is described by eqn. (3) where $k_{GH} = (6.75 \pm 0.05) \times 10^{-3}\ M^{-3}\ s^{-1}$. The complete rate law for the oxidation of Glc1Me by Cr^{VI} is then given by eqn. (4).

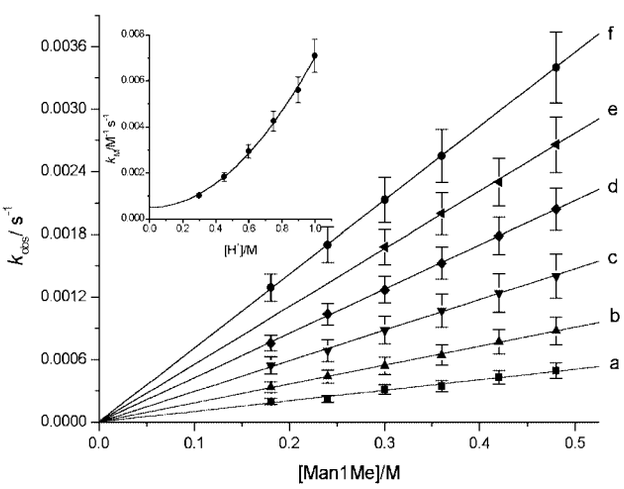

Fig. 1 Effect of [Man1Me] on k_{obs} at 40 °C, $I = 1.0$ M and $[H^+]$ (M): (a) 0.3; (b) 0.45; (c) 0.6; (d) 0.75; (e) 0.9; (f) 1.0. Inset: effect of acidity on k_M.

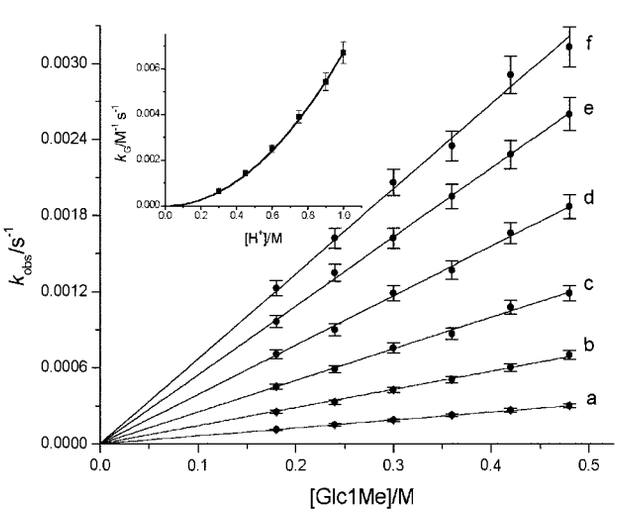

Fig. 2 Effect of [Glc1Me] on k_{obs} at 40 °C, $I = 1.0$ M and $[H^+]$ (M): (a) 0.3; (b) 0.45; (c) 0.6; (d) 0.75; (e) 0.9; (f) 1.0. Inset: effect of acidity on k_G.

$$k_G = k_{GH}\,[H^+]^2 \qquad (3)$$

$$-d[Cr^{VI}]/dt = k_{obs}[Cr^{VI}]_T = k_{GH}[H^+]^2[Glc1Me][Cr^{VI}]_T \qquad (4)$$

Detection of intermediate Cr^{V} by EPR spectroscopy

We have performed the reaction of Man1Me and Cr^{VI} at $[H^+]$ lower than used in the kinetic measurements in order to obtain information on the structure of chromium(v) species formed as intermediates in the reduction of Cr^{VI} to Cr^{III}. When the pH > 1, the redox reaction becomes slow and chromium(v) species remain in solution for a long time and the distribution and structure of these intermediates may be analysed from the EPR spectral features. The study was only made with Man1Me because this ligand affords chromium(v) chelates with well resolved EPR spectral signals. On the contrary, the EPR signals observed with Glc1Me are of low intensity and poorly resolved, probably due to the low ability of this ligand for binding to Cr^{V}.

In the 4–5 pH range and Man1Me : Cr^{VI} ratios of 5 : 1 to 20 : 1, at 25 °C, the EPR spectrum is composed (signals were deconvoluted by fitting the spectra by Lorentzian derivatives) of one triplet at $g_1 = 1.9800$ and one doublet at $g_2 = 1.9798$, each with the four weak ^{53}Cr (9.55% abundance, $I = 3/2$) hyperfine peaks at $16.5(3) \times 10^{-4}$ cm^{-1} spacing (Fig. 3, Table 3). At pH 3 and ligand to metal ratios up to 10 : 1, the spectra consist of one triplet at $g_1 = 1.9800$, one doublet at $g_2 = 1.9798$ and a shoulder with non-resolved superhyperfine (shf) pattern at $g_3 = 1.9788$ (Fig. 3). When the ligand to metal ratio is increased (≥20 : 1) the shoulder disappears. At pH 1 and 10 : 1 ligand : Cr^{VI} ratio, the EPR spectrum is composed of the triplet at $g_1 = 1.9800$, the doublet at g_2 1.9798 and the shoulder at g_3 1.9788, and two additional signals at g_4 1.9746 and g_5 1.9716 (Fig. 4). The intensity of signals at g_4 and g_5 relative to that of g_1, g_2 and g_3 increases with higher $[H^+]$.

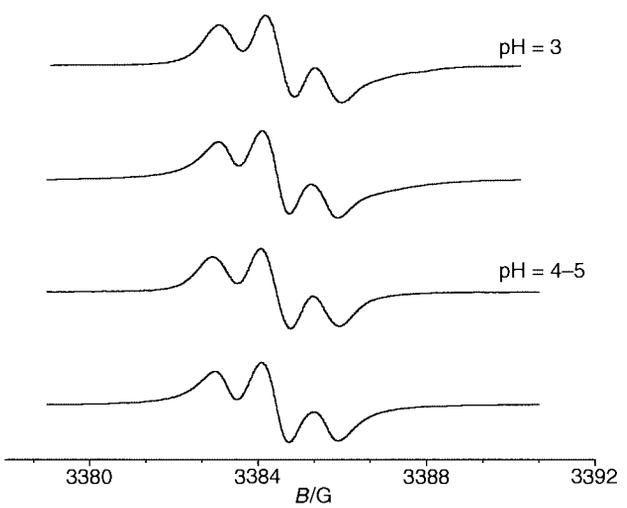

Fig. 3 X-Band EPR signal of a mixture of Man1Me and Cr^{VI} (10 : 1 ratio) at 25 °C, 1 day after mixing (modulation amplitude = 0.103 G, centre field = 3385 G, frequency 9.3677 GHz) and the simulated spectra.

Table 2 Values of k_M and k_G for different $[HClO_4]$

$[HClO_4]$/M	0.3	0.45	0.6	0.75	0.9	1.0
$10^4 k_M/M^{-1}\ s^{-1}$	10.1	18.2	29.4	42.5	55.3	70.9
$10^4 k_G/M^{-1}\ s^{-1}$	6.26	14.3	25.0	38.9	54.3	67.0

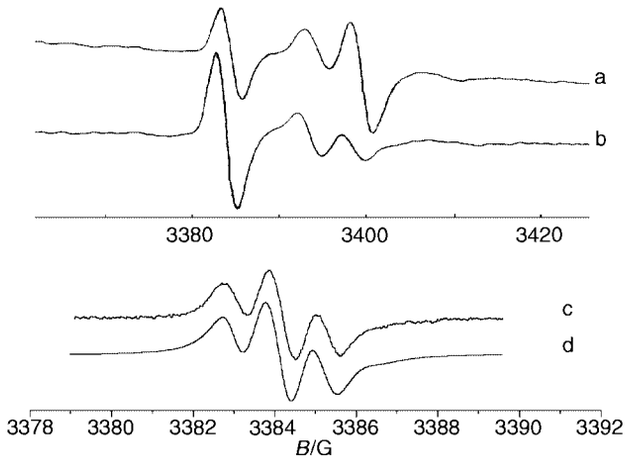

Fig. 4 X-Band EPR signal of a mixture of Man1Me and Cr^{VI} (10 : 1 ratio) at 25 °C, centre field 3385 G, frequency 9.3677 GHz. (a) $[H^+] = 0.3$ M, modulation amplitude 0.408 G. (b) $[H^+] = 0.1$ M, modulation amplitude 0.408 G. (c) $[H^+] = 0.1$ M, modulation amplitude 0.103 G. (d) Simulated spectrum.

Discussion

Mechanism of the Cr^{VI} oxidation

The rate laws for the oxidation of Man1Me and Glc1Me by Cr^{VI} show substrate first-order dependence, but they differ in that, for Man1Me, a term independent of $[H^+]$ is observed. These two terms in the rate law (eqn. (2)) for Man1Me indicate that there are at least two transition states, differing in composition but similar in energy, through which the reduction of Cr^{VI} can proceed by two parallel slow steps leading to the redox products. Interestingly, the kinetic parameters corresponding to the $[H^+]$ dependent path (k_{GH} and k_{MH}) are of the same order of magnitude. This should be related to the similar structure of the intermediate complex precursor of the redox steps formed with both substrates. Besides, in the range of substrate concentrations employed, both, Man1Me and Glc1Me, yield the methyl glycofuranurono-6,3-lactone as the only detected reaction product. In Scheme 2 a mechanism taking account of these facts is proposed for the chromium(VI) oxidation of Man1Me and Glc1Me. In the $[H^+]$ range under study, Cr^{VI} may exist as $HCrO_4^-$,[41] and it is known that the chromium(VI) oxidations are preceded by the formation of a chromate ester within which the electron transfer process takes place.[42,43] Thus, the first step of the mechanism proposed in Scheme 2 may be interpreted as the formation of several linkage isomers of the Gly1Me–Cr^{VI} monochelate[14] with the methyl glycoside acting as a bidentate ligand bound to Cr^{VI} *via* any pair of properly disposed hydroxyl groups. Four linkage isomers of general formula $[Cr(O)_2(Gly1MeH_{-2})(OH)(OH_2)]^-$ might be formed by co-ordination of the methyl glycoside with Cr^{VI} at the 2,3-, 3,4-, 3,6- or 4,6-diolate moiety (**I**–**IV**). Increase of the absorbance at 350 nm immediately after mixing may be evidence for the formation of these intermediate chromium(VI) complexes (Fig. S3

Table 3 EPR spectral parameters

Chromium(v) species	g_{iso}	$A_{iso}/10^4\ cm^{-1}$	$a_H/10^4\ cm^{-1}$ $(N)^a$
$[Cr(O)(O^2,O^3\text{-Man1Me})_2]^-$	1.9800	16.5	1.03(2)
$[Cr(O)(O^2,O^3\text{-Man1Me})(O^3,O^4\text{-Man1Me})]^-$	1.9798	16.5	0.98(1)
$[Cr(O)(O^2,O^3\text{-Man1Me})(O^6,O^3\text{-Man1MeA})]^-$	1.9788	ND	ND
$[Cr(O)(O^6,O^3\text{-Man1MeA})(H_2O)_2]^+$	1.9746	ND	ND
$[Cr(O)(O^2,O^3\text{-Man1Me})(H_2O)_3]^+$	1.9716	ND	ND

^{a} N = number of equivalent protons; ND = not determined.

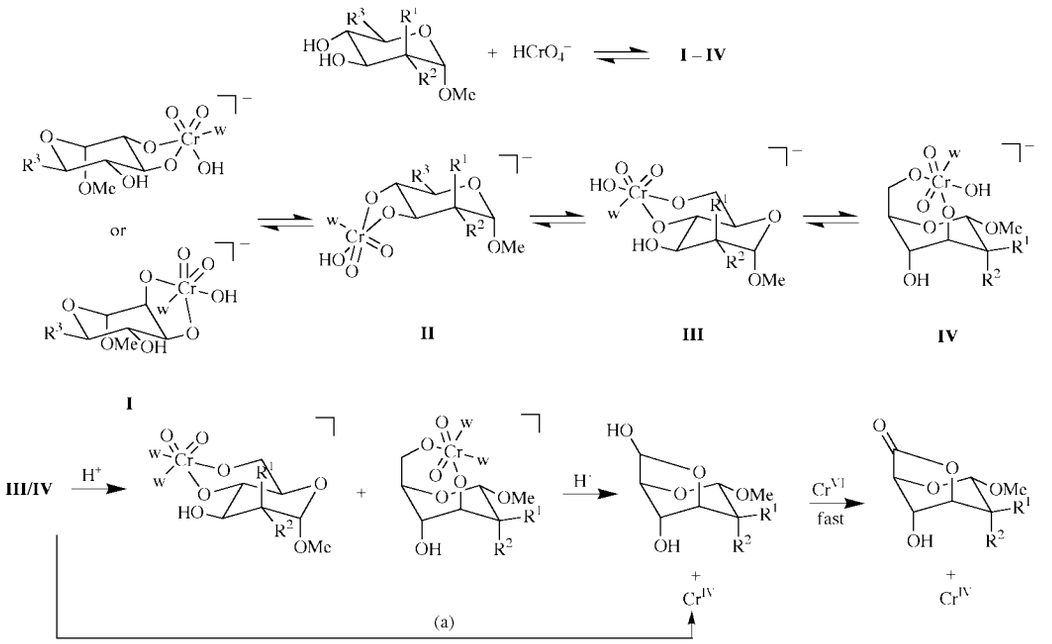

Scheme 2 For the reaction of Man1Me with Cr^{VI}, $R^1 = OH$, $R^2 = H$, $R^3 = CH_2OH$. For the reaction of Glc1Me with Cr^{VI}, $R^1 = H$, $R^2 = OH$, $R^3 = CH_2OH$, w = water. Step (a) only observed in the redox reaction of Man1Me with Cr^{VI}.

and S4, ESI data).† A different spectral pattern is observed when chromium(V) species forms and decays as fast as Cr^{VI}, and interfere with the chromium(V) absorbance.[16,25,26] The molar absorptivity of the stable chromium(V) complexes is lower than those corresponding to Cr^{VI} at the same $[H^+]$ (*i.e.* at $[H^+] = 0.3$ M, ε $[Cr^V(O)(ehba)_2]^-$, with ehba = 2-ethyl-2-hydroxybutanoic acid)[44] = 900 $dm^3\ mol^{-1}\ cm^{-1}$ and ε (Cr^{VI}) = 1375 $dm^3\ mol^{-1}\ cm^{-1}$). So, in those cases where Cr^V and Cr^{VI} decay at comparable rates, the absorbance of Cr^{VI} decreases slower than expected for a monotonic exponential decay, but the absorbance is never higher than that of the initial chromium(VI) solution (before the addition of the reductant), as observed in the present case. Taking into account that in the redox reaction only the primary alcohol is oxidised, it seems reasonable to think that the complex with the primary hydroxyl group bound to Cr^{VI} (**III** or **IV**) should be the precursor of the slow redox steps. In the case of the oxidation of Man1Me, intermediate **III** (and/or **IV**) yields directly the redox products (Cr^{IV} and methyl manno-hexodialdo-6,3-furanose-1,5-pyranoside) or protonates before affording the redox products through an acid catalysed redox step. In the reaction of Glc1Me with Cr^{VI} the redox reaction occurs only through the path involving protonation of the Glc1Me–Cr^{VI} ester prior to the acid catalysed electron-transfer slow step.

Fast redox reactions

For either Man1Me or Glc1Me, after the slow redox steps, reactions (5)–(8) may take place where diald = methyl gluco-

$$\text{Gly1Me} + Cr^{IV} \longrightarrow \text{Gly1Me}^{\bullet} + Cr^{III} \quad (5)$$

$$\text{Gly1Me}^{\bullet} + Cr^{VI} \longrightarrow \text{diald} + Cr^{V} \quad (6)$$

$$\text{Gly1Me} + Cr^{V} \longrightarrow \text{diald} + Cr^{III} \quad (7)$$

$$\text{diald} + Cr^{VI} \longrightarrow \text{Gly1MeL} + Cr^{IV} \quad (8)$$

hexodialdo-6,3-furanose-1,5-pyranoside or methyl manno-hexodialdo-6,3-furanose-1,5-pyranoside and Gly1MeL = methyl D-glucofuranurono-6,3-lactone or methyl D-manno-furanurono-6,3-lactone. Chromium(IV) formed in the slow redox step reacts with an excess of glycoside to yield Cr^{III} and the methyl glycoside radical in a fast step. The formation of the glycoside radical is supported by the observed polymerisation after addition of acrylonitrile. The rapid reaction of the glycoside radical and Cr^{VI} affords Cr^V, which can further oxidise the methyl glycoside to yield the methyl hexodialdo-6,3-furanose-1,5-pyranoside and Cr^{III}. The methyl hexodialdo-6,3-furanose-1,5-pyranoside is rapidly oxidised by Cr^{VI} to the methyl glycofuranurono-6,3-lactone. The fast oxidation of the methyl hexodialdo-6,3-furanose-1,5-pyranoside to the methyl glycofuranurono-6,3-lactone (compared to the methyl glycosides redox rates) may be explained as follows. The hemiacetalic group is oxidised faster than the terminal hydroxyl group and any of the secondary cyclic hydroxyl groups of the starting glycoside (aldoses are oxidised specifically at C1 to yield the aldonic acid in equilibrium with the aldonolactone as the only reaction product).[16,19,21,26,27] Besides, the furanose ring favours oxidation *vs*. complexation processes as the consequence of the influence of the strain-induced instability of the chromate ester on the redox rate (furanoses react much faster than pyranoses[26–28]). As a general rule, the less "stable" the intermediate chromium(VI) complex, precursor of the redox steps, the lower the energy barrier to overcome in the slow electron transfer steps and, consequently, the faster the resulting reaction rate. Thus, the lower stability of the intermediate chromium(VI) ester formed with the furanosic hemiacetalic O^6H favours the fast oxidation of the methyl hexodialdo-6,3-furanose-1,5-pyranoside to yield the final glycofuranurono-6,3-lactone.

Structure of intermediate chromium(V) species

The EPR spectral parameters g_{iso} and A_{iso} values, together with the proton superhyperfine coupling, have been shown to be useful in determining the binding modes of sugars to Cr^V.[16,21,26,27,45] The compound Man1Me may bind Cr^V as a bidentate ligand *via* any pair of properly disposed hydroxyl groups to yield several linkage isomers. It is known that the five-membered chromium(V) chelates are the most favourably formed and that the CrO^{3+} ion shows a marked preference for binding to *cis*- rather than *trans*-diol groups of cyclic diols.[46–48] Man1Me posseses two potentially binding modes *via* the 2,3-*cis*- and the 3,4-*trans*-diolate moieties to afford five-membered chromium(V) species, while other species, involving 2,4- or 4,6-diolate moieties, should be minor or very reactive species. It has been shown that the EPR spectrum of a species formed between Cr^V and a *cis*-cyclic diol yields a doublet, since only one proton is in

the plane of the unpaired electron density of the Cr^{V}; and the EPR spectrum of a Cr^{V}–*trans*-cyclic diol (with no protons lying in the ligand plane) yields a singlet.[46] Thus, the EPR spectral multiplicity of bis-chelate complexes formed between Cr^{V} and either *cis*- and *trans*-diol ligands will exhibit a triplet and singlet, respectively, arising from the orientation of the ring protons of the co-ordinated diol groups with respect to the basal plane of the complex.[46] Based on this, the EPR spectra of $[Cr(O)(O^2,O^3\text{-Man1Me})_2]^-$, $[Cr(O)(O^2,O^3\text{-Man1Me})(O^3,O^4\text{-Man1Me})]^-$ and $[Cr(O)(O^3,O^4\text{-Man1Me})_2]^-$ would exhibit a triplet, a doublet and a singlet, respectively, and the concentration of the singlet relative to the doublet and triplet is expected to be small. It has been determined that the g_{iso} and A_{iso} values of the EPR signals of chromium(v) complexes depend on the nature of the donor groups bound to Cr^{V} and the co-ordination number.[49–51] Thus, an estimation of the chromium(v) species in solution may be made according to the shf pattern together with the isotropic EPR parameters (g_{iso} and A_{iso}) based on the empirical method developed by Lay and co-workers.[49]

For the Man1Me–Cr^{V} system, in the 4–5 pH range (Fig. 3, Table 3), the g_{iso} (g_1 = 1.9800 (triplet) and g_2 = 1.9798 (doublet)) and A_{iso} ($16.5(3) \times 10^{-4}$ cm^{-1}) values of the chromium(v) EPR signals correspond to those calculated for five-co-ordinate oxochromate(v) complexes with four alcoholato donors. The different shf patterns indicate that they are two different linkage isomers of the chromium(v) bis-chelate ($[Cr(O)(O^2,O^3\text{-Man1Me})_2]^-$ and $[Cr(O)(O^2,O^3\text{-Man1Me})(O^3,O^4\text{-Man1Me})]^-$) or they correspond to bis- and mono-chelate $[Cr(O)(O^2,O^3\text{-Man1Me})_2]^-$ and $[Cr(O)(O^2,O^3\text{-Man1Me})(H_2O)_2]^+$.[45] The second alternative was ruled out by examining the effect of the ligand concentration on the EPR signals at constant pH. We found that both of the signals are independent of the ligand concentration. The independence of the spectra on [Man1Me] indicates that all the species present have a chromium(v) co-ordination sphere saturated with respect to Man1Me. Besides, the relative intensity of the two signals was also independent of increasing the total [Man1Me] and [Cr^{VI}], with both the [Man1Me]:[Cr^{VI}] and the pH value kept constant. In the 3–5 pH range, the constancy of the g_1:g_2 ratio at any of the [Man1Me]:[Cr^{VI}] used is consistent with the species responsible for these signals being the bis-chelates **V** and **VI** ($R^3 = CH_2OH$). The dominance of the triplet (85%) over the doublet, and the absence of the singlet, are consistent with the preference of Cr^{V} to bind *cis*- rather than *trans*-diol groups.

At pH 3 and ligand to metal ratios up to 10:1, the spectra show the two signals attributed to $[Cr(O)(O^2,O^3\text{-Man1Me})_2]^-$ **V** and $[Cr(O)(O^2,O^3\text{-Man1Me})(O^3,O^4\text{-Man1Me})]^-$ **VI** and an additional shoulder with non-resolved shf pattern at g_3 = 1.9788 (Fig. 3). This shoulder disappears when the ligand to metal ratio is ≥20:1, and the spectrum is comprised of the triplet at g_1 and the doublet at g_2 in a 85:15 ratio, as observed at higher pH. The formation of the additional signal at g_{iso} 1.9788 in the Cr^{VI}/Man1Me reaction is opposed to the formation of the bis-diolate Cr^{V}–$Man1Me_2$ species which are invariant with pH and [ligand], and the g_3 value corresponds to a five-co-ordinate oxochromium(v) complex. The dependence of this minor signal on both the pH and the [ligand] is consistent with an oxochromium(v) species formed with Man1Me and the oxidation product (Man1MeL), with donation occurring *via* the 6-carboxylate-3-hydroxy and the 2,3-dihydroxy donor groups. The calculated g_{iso} (1.9791) for $[Cr(O)(O^2,O^3\text{-Man1Me})(O^6,O^3\text{-Man1MeA})]^-$ **VII**, (Man1MeA acid open form of Man1MeL) is in reasonable agreement with the observed g_{iso} value. Besides, co-ordination to the oxidised ligand is consistent with the fact that Cr^{VI} is a stronger oxidant in more acidic media.

At pH 1 a more complex EPR spectral pattern is observed (Fig. 4). At this pH and 10:1 ligand:Cr^{VI} ratio, two additional signals at g_4 1.9746 and g_5 1.9716 appear together with the triplet at g_1 = 1.9800, the doublet at g_2 1.9798 and the shoulder at g_3 1.9788. The shf pattern of these two new signals is not resolved. However, we know they are pH dependent and the g_{iso} values can afford some information on their nature. The formation of the species at g_4 and g_5 is favoured by higher acid concentrations, and in 0.3 M $HClO_4$ the signal at g_5 is the dominant one (Fig. 4). The low g_{iso} value of this species suggests the presence of six-co-ordinate oxochromium(v) species, possibly $[Cr(O)(O^2,O^3\text{-Man1Me})(H_2O)_3]^+$ **VIII**. The calculated g_{iso} value for a six-co-ordinate oxochromium(v) species with two alcoholato donors and three water molecules (1.9724) is in reasonable agreement with the observed g_{iso} value. The positive charge of this species is also consistent with its appearance at high [H^+]. The intensity of the signal at g_4 (relative to $g_1 + g_2 + g_3$) increases at higher [H^+] and may be attributed to another positively charged monochelate $[Cr(O)(O^6,O^3\text{-Man1MeA})(H_2O)_2]^+$ **IX** (g_{calc} 1.9758) with donation occurring *via* the carboxylato and the 3-alcoholato groups of the oxidised product. The chromium(v) mono-chelates **VIII** and **IX** are possibly responsible for the higher rates observed for the Cr^{V}–glycoside redox reactions at pH < 1. At higher pH, where chromium(v) monochelates are not observed, chromium(v) complexes are stable enough to remain in solution for several days to months.

The ultimate fate of the chromium in these reactions is a chromium(III) species and a typical broad chromium(III) EPR signal centred at $g \approx 1.98$ is always observed at later time points.

Conclusion

In the studied reactions, the $Cr^{VI} \longrightarrow Cr^{III}$ reduction involves $Cr^{VI} \longrightarrow Cr^{IV} \longrightarrow Cr^{III}$ and $Cr^{VI} \longrightarrow Cr^{V} \longrightarrow Cr^{III}$ paths, with the $Cr^{VI} \longrightarrow Cr^{IV}$ step being the rate determining one. Compounds Glc1Me and Man1Me differ in the relative configuration of C2, but they are both oxidised specifically at C6 with very close reaction rates. However, Man1Me reduces Cr^{VI} to Cr^{IV} through two parallel paths while Glc1Me reduces Cr^{VI} only through an acidity dependent path. In both cases, a high [H^+] favours the formation of the redox products in a short time, but at pH > 1 the reaction of Glc1Me with Cr^{VI}

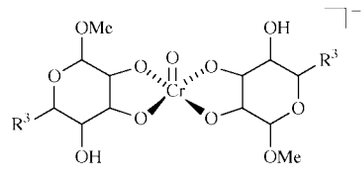

V

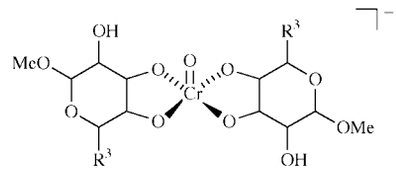

VI

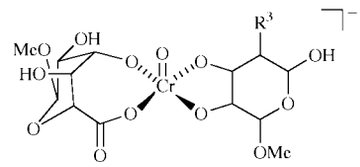

VII

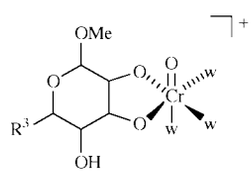

VIII

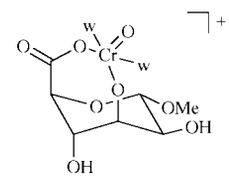

IX

is extremely slow as a consequence of the absence of a path independent of the $[H^+]$ to yield the redox products. Even when the reaction of Man1Me with Cr^{VI} is slow at pH > 1, it occurs through the $[H^+]$ independent path (*i.e.* for $[H^+] = 1 \times 10^{-3}$ M, $k_{M0} = 5 \times 10^{-4}$ M^{-1} s^{-1}, $k_{MH}[H^+]^2 = 6.75 \times 10^{-9}$ M^{-3} s^{-1} and $k_{GH}[H^+]^2 = 6.5 \times 10^{-9}$ M^{-3} s^{-1}) at a measurable rate. This fact (added to the lower ability of Glc1Me to yield chromium(v) complexes) contributes to the easier observation of the chromium(v) EPR signal for Man1Me than Glc1Me. At the high $[H^+]$ used in the kinetics measurements, positively charged chromium(v) monochelates form, and are believed to be the responsible for the fast decrease of the EPR chromium(v) signal in the 0.3–1 M $[H^+]$ range.

Acknowledgements

We thank the National Research Council of Argentina (CONICET), the Third World Academy of Sciences (TWAS), the National University of Rosario (UNR), the International Foundation for Sciences (IFS), the National Agency for Sciences Promotion (FONCyT) and ANTORCHAS Foundation for financial support.

References

1 C. B. Klein, in *Toxicology of Metals*, ed. L. W. Chang, CRC-Lewis Publishers, New York, 1996, pp. 205–220.
2 M. Costa, *Crit. Rev. Toxicol.*, 1997, **27**, 431.
3 S. A. Katz and H. Salem, *The Biological and Environmental Chemistry of Chromium*, VCH Publishers Inc., New York, 1994, pp. 65–119.
4 D. H. Stearns and K. E. Wetterhahn, *Chem. Res. Toxicol.*, 1994, **7**, 219.
5 K. E. Wetterhahn Jennette, *J. Am. Chem. Soc.*, 1982, **104**, 874.
6 P. O'Brien, J. Barrett and F. Swanson, *Inorg. Chim. Acta*, 1985, **108**, L19.
7 P. A. Lay and A. Levina, *J. Am. Chem. Soc.*, 1998, **120**, 6704.
8 M. Ciéslak-Golonka, *Polyhedron*, 1996, **15**, 3667.
9 M. Krumpolc, B. G. de Boer and J. Rocek, *J. Am. Chem. Soc.*, 1978, **100**, 145.
10 S. L. Brauer and K. E. Wetterhahn, *J. Am. Chem. Soc.*, 1991, **113**, 3001.
11 D. M. L. Goodgame, P. B. Hayman and D. E. Hathaway, *Polyhedron*, 1982, **1**, 497.
12 D. M. L. Goodgame and A. M. Joy, *J. Inorg. Biochem.*, 1986, **26**, 219.
13 R. Codd, P. A. Lay and A. Levina, *Inorg. Chem.*, 1997, **36**, 5440.
14 R. P. Farrell, P. A. Lay, A. Levina, I. A. Maxwell, R. Bramley, S. Brumby and J. Ji, *Inorg. Chem.*, 1998, **37**, 3159.
15 R. N. Bose, B. Fonkeng, G. Barr-David, R. P. Farrell, R. J. Judd, P. A. Lay and D. F. Sangster, *J. Am. Chem. Soc.*, 1996, **118**, 7139.
16 L. F. Sala, S. R. Signorella, M. Rizzotto, M. I. Frascaroli and F. Gandolfo, *Can. J. Chem.*, 1992, **70**, 2046.
17 S. Signorella, S. García and L. F. Sala, *Polyhedron*, 1992, **11**, 1391.
18 S. R. Signorella, M. I. Santoro, M. N. Mulero and L. F. Sala, *Can. J. Chem.*, 1994, **72**, 398.
19 M. Rizzotto, S. Signorella, M. I. Frascaroli, V. Daier and L. F. Sala, *J. Carbohydr. Chem.*, 1995, **14**, 45.
20 L. F. Sala, C. Palopoli and S. Signorella, *Polyhedron*, 1995, **14**, 1725.
21 S. Signorella, M. Rizzotto, V. Daier, M. I. Frascaroli, C. Palopoli, D. Martino, A. Bousseckson and L. F. Sala, *J. Chem. Soc.*, *Dalton Trans.*, 1996, 1607.
22 M. Rizzotto, M. I. Frascaroli, S. Signorella and L. F. Sala, *Polyhedron*, 1996, **15**, 1517.
23 S. Signorella, S. García and L. F. Sala, *Polyhedron*, 1997, **16**, 701.
24 C. Palopoli, S. Signorella and L. F. Sala, *New J. Chem.*, 1997, **21**, 343.
25 S. Signorella, M. Santoro, C. Palopoli, C. Brondino, J. M. Salas-Peregrin, M. Quirós and L. F. Sala, *Polyhedron*, 1998, **17**, 2739.
26 V. Daier, S. Signorella, M. Rizzotto, M. I. Frascaroli, C. Palopoli, C. Brondino, J. M. Salas-Peregrin and L. F. Sala, *Can. J. Chem.*, 1999, **77**, 57.
27 S. Signorella, V. Daier, S. García, R. Cargnello, J. C. González, M. Rizzotto and L. F. Sala, *Carbohydr. Res.*, 1999, **316**, 14.
28 S. Signorella, S. García and L. F. Sala, *J. Chem. Educ.*, 1999, **76**, 405.
29 J. B. Pridham, *Adv. Carbohydr. Chem.*, 1965, **20**, 371.
30 L. J. Haynes, *Adv. Carbohydr. Chem.*, 1963, **18**, 227; 1965, **20**, 357.
31 T. Reichstein, *Angew. Chem.*, *Int. Ed. Engl.*, 1962, **1**, 572.
32 R. J. McIlroy, in *The Plant Glycosides*, Longmans and Green, New York, 1951.
33 I. M. Kolthoff, E. B. Sandell, E. J. Meehan and S. Bruckenstein, in *Análisis Químico Cuantitativo*, Editorial S. R. L. Nigar, Buenos Aires, Sexta Edición, 1988, pp. 806–807.
34 E. M. Osman, K. C. Hobbs and W. E. Walston, *J. Am. Chem. Soc.*, 1951, **73**, 2726.
35 K. K. Sen Gupta, S. Sen Gupta, S. Kumar Mandal and A. Mahapatra, *J. Chem. Res.*, 1990, 60.
36 F. D. Snell and C. T. Snell, in *Colorimetric Methods of Analysis*, van Norstrand, New York, 1961, vol. IIIB, p. 353.
37 S. Signorella, M. Santoro, A. Frutos, G. Escandar, J. M. Salas Peregrin, V. Moreno, M. González Sierra and L. F. Sala, *J. Inorg. Biochem.*, 1999, **73**, 93.
38 W. Chandler, E. Lee and D. Lee, *J. Chem. Educ.*, 1987, **64**, 878.
39 WinSIM EPR calculations for MS-Windows, version 0.96, National Institute of Environmental Health Sciences, 111 Alexander Drive, Research Triangle Park, NC 27709, USA, 1995.
40 G. Haight, G. Jwisich, M. Kelso and P. Merril, *Inorg. Chem.*, 1985, **24**, 2740.
41 N. E. Brasch, D. A. Buckingham, A. B. Evans and C. R. Clark, *J. Am. Chem. Soc.*, 1996, **118**, 7969.
42 J. K. Beattie and G. P. Haight, in *Inorganic Reaction Mechanisms*, Part II, ed. J. O. Edwards, Wiley, New York, 1972.
43 M. Mitewa and P. Bontchev, *Coord. Chem. Rev.*, 1985, **61**, 241.
44 M. Krumpolc and J. Rocek, *Inorg. Synth.*, 1980, **20**, 63.
45 M. Branca, A. Dessí, H. Kozlowski, G. Micera and J. Swiatek, *J. Inorg. Biochem.*, 1990, **39**, 217.
46 R. Codd and P. A. Lay, *J. Am. Chem. Soc.*, 1999, **121**, 7864.
47 S. P. Kaiwar, M. S. S. Raghavan and C. P. Rao, *Carbohydr. Res.*, 1994, **256**, 29.
48 M. Branca, G. Micera and A. Dessi, *Inorg. Chim. Acta*, 1988, **153**, 61.
49 G. Barr-David, M. Charara, R. Codd, R. P. Farrell, J. A. Irwin, P. A. Lay, R. Bramley, S. Brumby, J. Y. Ji and G. R. Hanson, *J. Chem. Soc.*, *Faraday Trans.*, 1995, 1207.
50 R. Bramley, J. Y. Ji, R. J. Judd and P. A. Lay, *Inorg. Chem.*, 1990, **29**, 3089.
51 R. P. Farrell, R. J. Judd, P. A. Lay, R. Bramley and J. Y. Ji, *Inorg. Chem.*, 1989, **28**, 3401.